ACS Medicinal Chemistry Letters
Cite This: ACS Med. Chem. Lett. 2019, 10, 936−940
Letter
pubs.acs.org/acsmedchemlett

High in Vitro and in Vivo Tumor-Selective Novel Ruthenium(II) Complexes with 3-(2′-Benzimidazolyl)-7-fluoro-coumarin

Qi-Pin Qin,*[,†] Zhen-Feng Wang,[†] Xiao-Ling Huang,[†] Ming-Xiong Tan,*[,†] Bei-Bei Shi,[†] and Hong Liang*[,‡]

[†]Guangxi Key Lab of Agricultural Resources Chemistry and Biotechnology, College of Chemistry and Food Science, Yulin Normal University, 1303 Jiaoyudong Road, Yulin 537000, PR China

[‡]State Key Laboratory for the Chemistry and Molecular Engineering of Medicinal Resources, School of Chemistry and Pharmacy, Guangxi Normal University, 15 Yucai Road, Guilin 541004, PR China

Supporting Information

ABSTRACT: Three novel Ru(II) complexes, namely, $(RuCl_2[L^a][DMSO]_2)\cdot H_2O$ (**Ru1**), $(RuCl_2[L^b][DMSO]_2)$ (**Ru2**), and $(RuCl_2[L^c][DMSO]_2)$ (**Ru3**), which respectively contain 3-(2′-benzimidazolyl)coumarin (L^a), 3-(2′-benzimidazolyl)-7-fluoro-coumarin (L^b), and 3-(2′-benzimidazolyl)-7-methoxyl-coumarin (L^c), were first designed and characterized. **Ru2** showed potent antitumor activity against NCI-H460 cells (IC_{50} = 0.30 ± 0.02 μM) and high selectivity between NCI-H460 cancer cells and normal HL-7702 cells. **Ru2** induced NCI-H460 apoptosis via telomerase inhibition, which involved DNA damage, cell-cycle distribution, and S phase-protein down-regulation. However, **Ru1** did not demonstrate such effects in NCI-H460 cells, which is undoubtedly associated with the key regulatory role of the 7-fluoro substituted group in the L^b ligand of **Ru2**. **Ru2** exhibited considerably higher anticancer efficacy (inhibition rate [IR] = 61.3%) compared with cisplatin (IR= 25.5%) in a NCI-H460 xenograft mouse model. Thus, this coumarin Ru(II) compound is a promising **Ru2**-targeting telomerase anticancer agent.

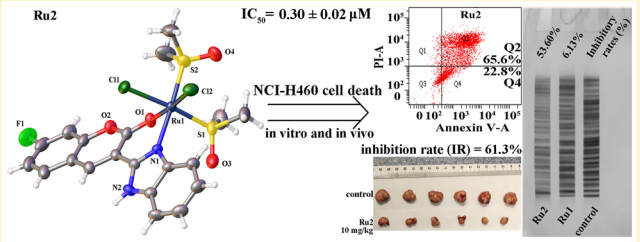

KEYWORDS: *3-(2′-Benzimidazolyl)-7-fluoro-coumarin, Ru(II) complex, telomerase, anticancer activity, cell cycle distribution*

Ru(II) complexes exhibit high water solubility and low general toxicity compared with cisplatin and its derivatives, such as oxaliplatin and carboplatin.[1−24] Many Ru(II) compounds, such as NAMI-A,[5−7] DW1/2,[8,9] KP1019 and KP1339,[3,10−13,20] RM175,[11−16] RAPTA-T and RAPTA complexes (Figure S1),[2,17,18] ($[Ru\{phen\}_2]_2tpphz$),[4+,19] three water-soluble chiral 4-(2,3-dihydroxypropyl)-formamide oxoporphine Ru(II) complexes,[21] Δ-/Λ-$(Ru[phen]_2[p\text{-}MOPIP])^{2+}$, and Λ-/Δ-$(Ru[phen]_2[p\text{-}HPIP])^{2+}$ complexes,[22,23] display high antitumor activity. Thus, Ru(II/III) compounds must be designed to understand in vitro and in vivo apoptosis mechanisms.

Various coumarin derivatives and their metal complexes exhibit a wide range of anti-HIV, antimicrobial, anticancer, antiviral, and anti-Alzheimer activities.[25−35] However, Ru(II) complexes with 3-(2′-benzimidazolyl)coumarin derivatives (BMC, FBMC, and MBMC) have not been reported, and the detailed antitumor mechanisms of Ru(II) compounds remain unexplored.

Thus, we first designed three novel Ru(II) complexes, namely, $(RuCl_2[L^a][DMSO]_2)\cdot H_2O$ (**Ru1**), $(RuCl_2[L^b][DMSO]_2)$ (**Ru2**), and $(RuCl_2[L^c][DMSO]_2)$ (**Ru3**), which contain 3-(2′-benzimidazolyl)coumarin (L^a), 3-(2′-benzimidazolyl)-7-fluoro-coumarin (L^b), and 3-(2′-benzimidazolyl)-7-methoxyl-coumarin (L^c), respectively. Furthermore, we proposed a possible in vitro and in vivo anticancer mechanism.

Three new coumarin derivatives, Ru(II) complexes **Ru1**−**Ru3**, were first synthesized with 2-cyanomethylbenzimidazole as the starting material (Scheme S1). The synthesized L^a−L^c and **Ru1**−**Ru3** were characterized via electrospray mass spectrometry (ESI-MS), single-crystal X-ray diffraction, elemental analysis, and infrared spectroscopy (Figures S1−S10). As shown in Figures 1, S11, and S12, the Ru(II) ion in **Ru1**−**Ru3** adopted an octahedral environment. The solution behavior of **Ru1**−**Ru3** (2.0×10^{-5} M) in Tris-HCl buffer (10 mM, pH = 7.35) was further studied by UV−vis absorption spectra. As shown in Figure S13, the time-dependent (0, 24, and 48 h) UV−vis spectra of **Ru1**−**Ru3** (2.0×10^{-5} M) suggest that **Ru1**−**Ru3** were stable in 10 mM Tris-HCl buffer for 48 h at 37 °C.

The cytotoxicity of L^a−L^c, *cis*-$RuCl_2(DMSO)_4$, cisplatin, and **Ru1**−**Ru3** against human cancer cells (NCI-H460, T-24, SK-OV-3, MGC80-3, and A549) and normal cells (HL-7702) was investigated by MTT assays. As shown in Tables S10 and 1, **Ru1**−**Ru3** did not exhibit cytotoxicity in T-24, SK-OV-3, MGC80-3, A549, and HL-7702 cell lines. The IC_{50} values determined for **Ru2** were lower (IC_{50} = 0.30 ± 0.02 μM) than

Received: March 10, 2019
Accepted: May 21, 2019
Published: May 22, 2019

DOI: 10.1021/acsmedchemlett.9b00098
ACS Med. Chem. Lett. 2019, 10, 936−940

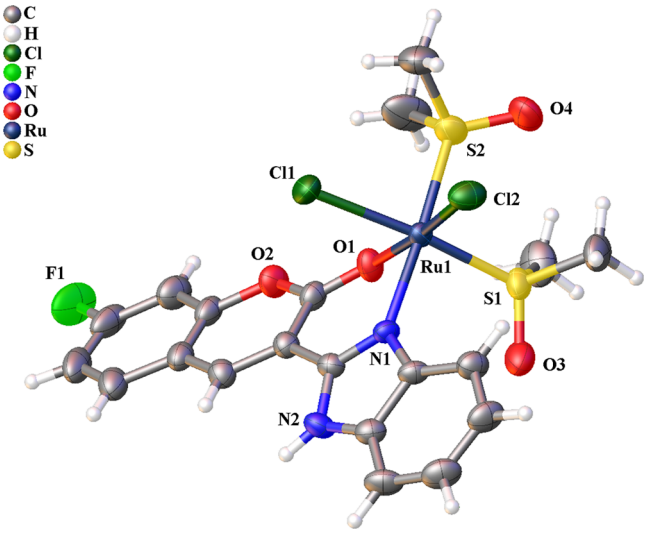

Figure 1. Crystal structures of **Ru2**.

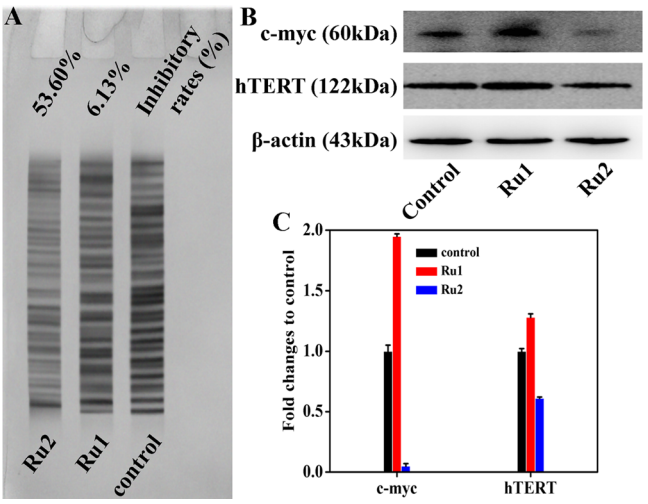

Figure 2. Ru2 (0.30 μM) and **Ru1** (15.78 μM) inhibited telomerase activity in NCI-H460 cells for 24 h. (A) Telomerase activity assay. (B and C) Levels of c-myc/hTRET in **Ru2** (0.30 μM)- and **Ru1** (15.78 μM)-treated cells.

those for L^a–L^c, *cis*-$RuCl_2(DMSO)_4$ (RuD), **Ru1**, **Ru3**, and cisplatin and followed the order of **Ru2** > **Ru3** > cisplatin > **Ru1**. **Ru2** demonstrated remarkable antitumor activity against NCI-H460 cells that was higher than or close to that in previous reports.[5−24,36,37] Therefore, NCI-H460 cells were selected for further study on the cell death mechanism induced by **Ru2** (0.30 μM) and **Ru1** (15.78 μM).

To explore the apoptosis mechanism of **Ru2** (0.30 μM) and **Ru1** (15.78 μM), we performed an ICP-MS (cellular uptake) study.[36−38] Table S11 shows the incubation and treatment of NCI-H460 cells with **Ru2** (0.30 μM) and **Ru1** (15.78 μM). The concentration of Ru(II) inside these cancer cells and nuclear fraction for **Ru2** ([4.58 ± 0.11 nmol of Ru]/10^6 cells) at 0.30 μM was more than that for **Ru1** ([1.56 ± 0.14 nmol of Ru]/10^6 cells), oxoaporphine Ru(II) complex ([3.81 ± 0.14 nmol Ru]/10^6 cells), and cisplatin ([2.08 ± 0.11 nmol Pt]/10^6 cells).[21,37] C-myc, telomerase, and hTERT play a crucial role in cancer cell growth or apoptosis.[33,39−50] In the current study, TRAP-silver staining[33,39−41] assays showed that **Ru2** (0.30 μM) exhibited more effective inhibition (53.60%, Figure 2) toward telomerase activity compared with **Ru1** (6.13%). As expected, the level of c-myc/hTERT protein in NCI-H460 cells was reduced in **Ru2** (0.30 μM) but was increased in **Ru1** (15.78 μM) compared with the control. A possible mechanism of **Ru1** (15.78 μM) is the direct activation of the c-myc/hTERT protein by c-myc before c-myc binds to E-box and telomerase inhibitor, and such activation was not related to cell apoptosis, which was consistent with the reports of Chen et al.[21,37] The telomerase inhibition of **Ru2** (0.30 μM) may be different from that of **Ru1** (15.78 μM) in the NCI-H460 cells.

Telomerase inhibition by each drug/compound may lead to cell cycle arrest at the S phase and DNA damage.[42−44] As shown in Figure S14, **Ru2** (0.30 μM)-treated cells exhibited an increased number of cells (46.98%) at the S phase compared with the control (36.68%). This phenomenon remarkably caused DNA damage (Figure 3), consequently increasing the level of H2A.X and cleaved-PARP proteins and decreasing that of cyclin A2 and CDK2 (Figure S15). By contrast, **Ru1** (15.78 μM) demonstrated less effect on NCI-H460 cells.

Subsequently, we investigated whether **Ru2** (0.30 μM) and **Ru1** (15.78 μM) could induce apoptosis and inhibit the migration of NCI-H460 cells. **Ru2** (0.30 μM, ca. 88.4%) induced the apoptosis (Figure 4) of HeLa cells for 24 h to a greater extent than oxoaporphine Ru(II) complexes (ca. 20.2%−54.7%)[21,37] and **Ru1** (15.78 μM, ca. 18.9%). Cell migration was inhibited by **Ru2** (0.30 μM) and **Ru1** (15.78 μM) by ∼47.1% and 29.4% compared with the control cells, respectively (Figure S16). **Ru2** (0.30 μM) remarkably inhibited NCI-H460 cancer cell migration compared with **Ru1** (15.78 μM).

Ru2, which showed the highest solubility in solvent (5% v/v DMSO/saline), was used to preliminarily study its safety (Figure S17), and ICR mice were treated with possible maximal administration values (0.6 mL/20 g) by intra-

Table 1. IC_{50} Values (μM) of Each Compound against Selected Human Cell Lines[a]

	NCI-H460	T-24	SK-OV-3	MGC80-3	A549	HL-7702
L^a	>100	>150	>150	>100	>100	>100
Ru1	15.78 ± 1.02	53.01 ± 1.26	65.02 ± 1.12	91.03 ± 1.01	41.36 ± 0.99	>100
L^b	>100	>100	>100	>100	>100	>100
Ru2	0.30 ± 0.02	25.63 ± 1.44	35.69 ± 2.03	68.69 ± 1.15	20.14 ± 0.28	>100
L^c	>100	>100	>100	>100	>100	>100
Ru3	10.04 ± 0.73	30.00 ± 1.09	46.25 ± 1.59	88.24 ± 1.79	34.39 ± 1.05	>100
RuD	>100	>100	>100	>100	>100	>100
cisplatin[b]	13.25 ± 1.18	17.03 ± 0.57	15.09 ± 0.91	12.06 ± 1.18	12.36 ± 0.19	17.03 ± 1.06

[a]IC_{50} = mean ± SD (standard error of the mean, n = 5). These six human cancer and normal cells were treated with the ligands and each of the Ru complexes for 48 h. [b]Cisplatin (1.0 mM) was prepared in 0.154 M NaCl.

DOI: 10.1021/acsmedchemlett.9b00098
ACS Med. Chem. Lett. 2019, 10, 936−940

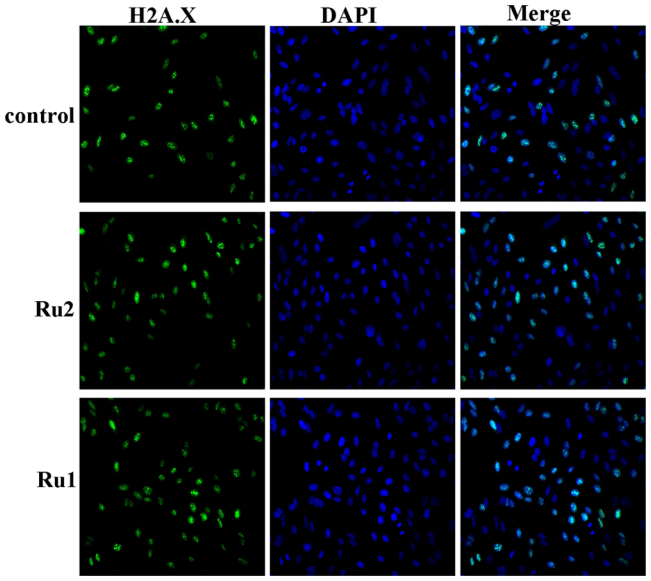

Figure 3. Effects of **Ru2** (0.30 μM) and **Ru1** (15.78 μM) on the level of H2A.X in NCI-H460 cells for 24 h. These cells were incubated with anti-H2A.X (primary antibodies) and Alexa Fluor 488 Goat Anti-Rabbit IgG (H+L, green, secondary antibody), stained with DAPI (blue), and examined by immunofluorescence (LeicaTCS-SP5 confocal microscope, Germany, 200× magnification).

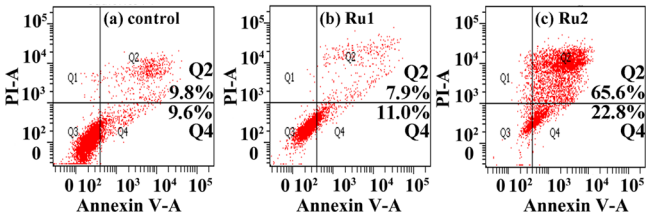

Figure 4. Apoptosis of NCI-H460 cells treated with (c) **Ru2** (0.30 μM) and (b) **Ru1** (15.78 μM) for 24 h compared with control (a).

peritoneal injection. No apparent body weight decrease (m_{start} = 19.03 ± 0.67 g; m_{end} = 21.33 ± 0.37 g) and injury condition (Figures S17 and 5; Tables S12−S14) were observed for **Ru2** (10.0 mg/kg every 2 days [q2z])-treated mice, demonstrating the low systemic toxicity of coumarin Ru(II) compound. The in vivo anticancer efficacy of **Ru2** (10.0 mg/kg q2d) on NCI-H460 cancer xenograft was analyzed. The NCI-H460 tumor inhibition rate (IR) was 61.3% for **Ru2** (Figure 5; Tables S12−S14), showing a higher anticancer efficiency compared with cisplatin (IR = 25.5%)[37,46,47] and oxoaporphine Ru(II) complex (IR = 53.3%).[21,37]

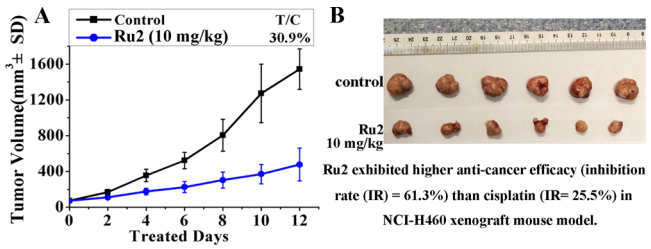

Figure 5. In vivo anticancer activity of **Ru2** in mice bearing NCI-H460 xenograft. Images (B) and changes (A) of tumors or volumes after intravenous injection.

In conclusion, we first designed the three novel Ru(II) complexes, namely, **Ru1**−**Ru3** containing 3-(2′-benzimidazolyl)coumarin derivatives. The most active compound, **Ru2**, showed higher cytotoxic potency against NCI-H460 cells (IC_{50} = 0.30 ± 0.02 μM) compared with cisplatin (13.25 ± 1.18 μM) and demonstrated high selectivity between NCI-H460 cancer cells and HL-7702 normal cells. Furthermore, **Ru2** accumulated preferentially in the nuclear fraction of NCI-H460 cells and induced their apoptosis via telomerase inhibition, DNA damage, and cell cycle distribution. The **Ru2** exhibited evident priority on antitumor activity than **Ru1**, which should be highly related to the key roles of the 7-fluoro substituted group in L^b ligand of **Ru2**. An in vivo study suggested that **Ru2** exhibited higher anticancer efficacy (IR = 61.3%) compared with cisplatin (IR = 25.5%) in the NCI-H460 xenograft. Therefore, this coumarin Ru(II) compound may be a promising **Ru2**-targeting telomerase anticancer agent.

■ ASSOCIATED CONTENT

Supporting Information

The Supporting Information is available free of charge on the ACS Publications website at DOI: 10.1021/acsmedchemlett.9b00098.

X-ray crystallization data of **Ru1**−**Ru3**. The CCDC numbers for **Ru1**−**Ru3** are 1902151−1902153 (ZIP)

Experimental procedures, Tables S1−S14, and Figures S1−S16. NMR, ESI-MS, IR, and experiments of **Ru1**−**Ru3** (PDF)

■ AUTHOR INFORMATION

Corresponding Authors

*Q.-P. Qin: Telephone and Fax: (086) 775-2623650, E-mail: qpqin2018@126.com.

*M.-X. Tan: Telephone and Fax: (086) 775-2623650, E-mail: mxtan2018@126.com.

*H. Liang: Telephone: (086) 773-2120998, Fax: (086) 773-21209958, hliang@gxnu.edu.cn.

ORCID

Qi-Pin Qin: 0000-0001-9596-4512

Ming-Xiong Tan: 0000-0002-5352-4030

Author Contributions

All authors contributed to the writing of this manuscript.

Funding

We thank the National Natural Science Foundation of China (Nos. 21867017 and 21761033), the Natural Science Foundation of Guangxi (No. 2018GXNSFBA138021), and the Innovative Team and Outstanding Talent Program of Colleges and Universities in Guangxi (2014-49 and 2017-38) for financial support.

Notes

The authors declare no competing financial interest.

■ ACKNOWLEDGMENTS

We acknowledge professors Fu-Ping Huang and Peng-Fei Yao for helping perform the X-ray crystallization data analysis of **Ru1**−**Ru3**.

■ ABBREVIATIONS

SD, standard deviation; RuD, *cis*-$RuCl_2(DMSO)_4$; ESI-MS, electrospray mass spectrometry; MTT, 3-(4,5-dimethylthiazol-

DOI: 10.1021/acsmedchemlett.9b00098
ACS Med. Chem. Lett. 2019, 10, 936−940

2-yl)-2,5-diphenyltetrazolium bromide; IR, tumor growth inhibition rate

REFERENCES

(1) Bruijnincx, P. C. A.; Sadler, P. J. New trends for metal complexes with anticancer activity. *Curr. Opin. Chem. Biol.* **2008**, *12*, 197−206.

(2) Zeng, L.; Gupta, P.; Chen, Y.; Wang, E.; Ji, L.; Chao, H.; Chen, Z.-S. The development of anticancer ruthenium(II) complexes: from single molecule compounds to nanomaterials. *Chem. Soc. Rev.* **2017**, *46*, 5771−5804.

(3) Timerbaev, A. R.; Hartinger, C. G.; Aleksenko, S. S.; Keppler, B. K. Interactions of antitumor metallodrugs with serum proteins: advances in characterization using modern analytical methodology. *Chem. Rev.* **2006**, *106*, 2224−2248.

(4) Fang, L.; Qin, X.; Zhao, J.; Gou, S. Construction of dual stimuli-responsive platinum(IV) hybrids with NQO1 targeting ability and overcoming cisplatin resistance. *Inorg. Chem.* **2019**, *58*, 2191−2200.

(5) Bergamo, A.; Gaiddon, C.; Schellens, J. H.; Beijnen, J. H.; Sava, G. Approaching tumour therapy beyond platinum drugs: status of the art and perspectives of ruthenium drug candidates. *J. Inorg. Biochem.* **2012**, *106*, 90−99.

(6) Rademaker-Lakhai, J. M.; van den Bongard, D.; Pluim, D.; Beijnen, J. H.; Schlens, J. M. H. A phase I and pharmacological study with imidazolium-trans-DMSO-imidazole-tetrachlororuthenate, a novel ruthenium anticancer agent. *Clin. Cancer Res.* **2004**, *10*, 3717−3727.

(7) Novohradsky, V.; Bergamo, A.; Cocchietto, M.; Zajac, J.; Brabec, V.; Mestroni, G.; Sava, G. Influence of the binding of reduced NAMI-A to human serum albumin on the pharmacokinetics and biological activity. *Dalton Trans* **2015**, *44*, 1905−1913.

(8) Smalley, K. S. M.; Contractor, R.; Haas, N. K.; Kup, A. N.; Atilla-Gokcuman, G. E.; Williams, D. S.; Bregman, H.; Flaherty, K. T.; Soengas, M. S.; Meggers, E.; Herlyn, M. An organometallic protein kinase inhibitor pharmacologically activates p53 and induces apoptosis in human melanoma cells. *Cancer Res.* **2007**, *67*, 209−217.

(9) Xie, P.; Streu, C.; Qin, J.; Bregman, H.; Pagano, N.; Meggers, E.; Marmorstein, R. The crystal structure of BRAF in complex with an organoruthenium inhibitor reveals a mechanism for inhibition of an active form of BRAF kinase. *Biochemistry* **2009**, *48*, 5187−5198.

(10) Bratsos, I.; Jedner, S.; Gianferrara, T.; Alessio, E. Ruthenium anticancer compounds: challenges and expectations. *Chimia* **2007**, *61*, 692−697.

(11) Meng, X.; Leyva, M. L.; Jenny, M.; Gross, I.; Benosman, S.; Fricker, B.; Harlepp, S.; Hébraud, P.; Boos, A.; Wlosik, P.; Bischoff, P.; Sirlin, C.; Pfeffer, M.; Loeffler, J. P.; Gaiddon, C. A ruthenium-containing organometallic compound reduces tumor growth through induction of the endoplasmic reticulum stress gene CHOP. *Cancer Res.* **2009**, *69*, 5458−5466.

(12) Hartinger, C. G.; Zorbas-Seifried, S.; Jakupec, M. A.; Kynast, B.; Zorbas, H.; Keppler, B. K. From bench to bedside-preclinical and early clinical development of the anticancer agent indazolium trans-[tetrachlorobis (1H-indazole) ruthenate(III)](KP1019 or FFC14A). *J. Inorg. Biochem.* **2006**, *100*, 891−904.

(13) Sadafi, F.-Z.; Massai, L.; Bartolommei, G.; Moncelli, M. R.; Messori, L.; Tadini-Buoninsegni, F. Anticancer ruthenium(III) complex KP1019 interferes with ATP-dependent Ca^{2+} translocation by sarco-endoplasmic reticulum Ca^{2+}-ATPase (SERCA). *ChemMedChem* **2014**, *9*, 1660−1664.

(14) Bergamo, A.; Masi, A.; Peacock, A. F.; Habtemariam, A.; Sadler, P. J.; Sava, G. In vivo tumour and metastasis reduction and in vitro effects on invasion assays of the ruthenium RM175 and osmium AFAP51 organometallics in the mammary cancer model. *J. Inorg. Biochem.* **2010**, *104*, 79−86.

(15) Morris, R. E.; Aird, R. E.; Murdoch, P. S.; Chen, H.; Cummings, J.; Hughes, N. D.; Parsons, S.; Parkin, A.; Boyd, G.; Jodrell, D. I.; Sadler, P. J. Inhibition of cancer cell growth by ruthenium(II) arene complexes. *J. Med. Chem.* **2001**, *44*, 3616−3621.

(16) Aird, R. E.; Cummings, J.; Ritchie, A. A.; Muir, M.; Morris, R. E.; Chen, H.; Sadler, P. J.; Jordrell, D. I. In vitro and in vivo activity and cross resistance profiles of novel ruthenium(II) organometallic arene complexes in human ovarian cancer. *Br. J. Cancer* **2002**, *86*, 1652−1657.

(17) Nowak-Sliwinska, P.; van Beijnum, J. R.; Casini, A.; Nazarov, A. A.; Wagnières, G.; van den Bergh, H.; Dyson, P. J.; Griffioen, A. W. Organometallic ruthenium(II) arene compounds with antiangiogenic activity. *J. Med. Chem.* **2011**, *54*, 3895−3902.

(18) Kilpin, K. J.; Cammack, S. M.; Clavel, C. M.; Dyson, P. J. Ruthenium(II) arene PTA (RAPTA) complexes: impact of enantiomerically pure chiral ligands. *Dalton Trans* **2013**, *42*, 2008−2014.

(19) Wilson, T.; Costa, P. J.; Félix, V.; Williamson, M. P.; Thomas, J. A. Structural studies on dinuclear ruthenium(II) complexes that bind diastereoselectively to an antiparallel folded human telomere sequence. *J. Med. Chem.* **2013**, *56*, 8674−8683.

(20) Hartinger, C. G.; Jakupec, M. A.; Zorbas-Seifried, S.; Groessl, M.; Egger, A.; Berger, W.; Zorbas, H.; Dyson, P. J.; Keppler, B. K. KP1019, a new redox-active anticancer agent-Preclinical development and results of a clinical phase I study in tumor patients. *Chem. Biodiversity* **2008**, *5*, 2140−2155.

(21) Chen, Z.-F.; Qin, Q.-P.; Qin, J.-L.; Zhou, J.; Li, Y.-L.; Li, N.; Liu, Y.-C.; Liang, H. Water-soluble ruthenium(II) complexes with chiral 4-(2, 3-dihydroxypropyl)-formamide oxoaporphine (FOA): in vitro and in vivo anticancer activity by stabilization of G-Quadruplex DNA, inhibition of telomerase activity, and induction of tumor cell apoptosis. *J. Med. Chem.* **2015**, *58*, 4771−4789.

(22) Sun, D.; Liu, Y.; Liu, D.; Zhang, R.; Yang, X.; Liu, J. Stabilization of G-quadruplex DNA, inhibition of telomerase activity and live cell imaging studies of chiral ruthenium(II) complexes. *Chem. - Eur. J.* **2012**, *18*, 4285−4295.

(23) Yu, Q.; Liu, Y.; Wang, C.; Sun, D.; Yang, X.; Liu, Y.; Liu, J. Chiral ruthenium(II) polypyridyl complexes: stabilization of g-quadruplex DNA, inhibition of telomerase activity and cellular uptake. *PLoS One* **2012**, *7*, No. e50902.

(24) Gill, M. R.; Thomas, J. A. Ruthenium(II) polypyridyl complexes and DNA-from structural probes to cellular imaging and therapeutics. *Chem. Soc. Rev.* **2012**, *41*, 3179−3192.

(25) Paul, K.; Bindal, S.; Luxami, V. Synthesis of new conjugated coumarin-benzimidazole hybrids and their anticancer activity. *Bioorg. Med. Chem. Lett.* **2013**, *23*, 3667−3672.

(26) Cosconati, S.; Rizzo, A.; Trotta, R.; Pagano, B.; Iachettini, S.; De Tito, S.; Lauri, I.; Fotticchia, I.; Giustiniano, M.; Marinelli, L.; Giancola, C.; Novellino, E.; Biroccio, A.; Randazzo, A. Shooting for selective drug-like G-quadruplex binders: evidence for telomeric DNA damage and tumor cell death. *J. Med. Chem.* **2012**, *55*, 9785−9792.

(27) Cosconati, S.; Marinelli, L.; Trotta, R.; Virno, A.; Mayol, L.; Novellino, E.; Olson, A. J.; Randazzo, A. Tandem application of virtual screening and NMR experiments in the discovery of brand new DNA quadruplex groove binders. *J. Am. Chem. Soc.* **2009**, *131*, 16336−16337.

(28) Wu, W.; Wu, W.; Ji, S.; Guo, H.; Zhao, J. Accessing the long-lived emissive 3IL triplet excited states of coumarin fluorophores by direct cyclometallation and its application for oxygen sensing and upconversion. *Dalton Trans* **2011**, *40*, 5953−5963.

(29) Christie, R. M.; Lui, C. H. Studies of fluorescent dyes: part 2. An investigation of the synthesis and electronic spectral properties of substituted 3-(2'-benzimidazolyl) coumarins. *Dyes Pigm.* **2000**, *47*, 79−89.

(30) Ali, M.; Dondaine, L.; Adolle, A.; Sampaio, C.; Chotard, F.; Richard, P.; Denat, F.; Bettaieb, A.; Le Gendre, P.; Laurens, V.; Goze, C.; Paul, C.; Bodio, E. Nticancer agents: does a phosphonium behave like a gold(I) phosphine complex? Let a "smart" probe answer! *J. Med. Chem.* **2015**, *58*, 4521−4528.

(31) Jung, H. S.; Kwon, P. S.; Lee, J. W.; Kim, J. I.; Hong, C. S.; Kim, J. W.; Yan, S.; Lee, J. Y.; Lee, J. H.; Joo, T.; Kim, J. S. Coumarin-derived Cu^{2+}-selective fluorescence sensor: synthesis, mechanisms, and applications in living cells. *J. Am. Chem. Soc.* **2009**, *131*, 2008−2012.

DOI: 10.1021/acsmedchemlett.9b00098
ACS Med. Chem. Lett. 2019, 10, 936−940

(32) Hanthorn, J. J.; Haidasz, E.; Gebhardt, P.; Pratt, D. A. A versatile fluorescence approach to kinetic studies of hydrocarbon autoxidations and their inhibition by radical-trapping antioxidants. *Chem. Commun.* **2012**, *48*, 10141−10143.
(33) Qin, Q.-P.; Wang, S.-L.; Tan, M.-X.; Wang, Z.-F.; Huang, X.-L.; Wei, Q.-M.; Shi, B.-B.; Zou, B.-Q.; Liang, H. Synthesis and antitumor mechanisms of two novel platinum(II) complexes with 3-(2′-benzimidazolyl)-7-methoxycoumarin. *Metallomics* **2018**, *10*, 1160−1169.
(34) Kostova, I.; Momekov, G. New cerium(III) complexes of coumarins-synthesis, characterization and cytotoxicity evaluation. *Eur. J. Med. Chem.* **2008**, *43*, 178−188.
(35) Li, M.-J.; Wong, K. M.-C.; Yi, C.; Yam, V. W.-W. New ruthenium(II) complexes functionalized with coumarin derivatives: synthesis, energy-transfer-based sensing of esterase, cytotoxicity, and imaging studies. *Chem. - Eur. J.* **2012**, *18*, 8724−8730.
(36) Pierroz, V.; Joshi, T.; Leonidova, A.; Mari, C.; Schur, J.; Ott, I.; Spiccia, L.; Ferrari, S.; Gasser, G. Molecular and cellular characterization of the biological effects of ruthenium(II) complexes incorporating 2-pyridyl-2-pyrimidine-4-carboxylic Acid. *J. Am. Chem. Soc.* **2012**, *134*, 20376−20387.
(37) Chen, Z.-F.; Qin, Q.-P.; Qin, J.-L.; Liu, Y.-C.; Huang, K.-B.; Li, Y.-L.; Meng, T.; Zhang, G.-H.; Peng, Y.; Luo, X.-J.; Liang, H. Stabilization of G-quadruplex DNA, inhibition of telomerase activity and tumor cell apoptosis of organoplatinum(II) complexes with oxoisoaporphine. *J. Med. Chem.* **2015**, *58*, 2159−2179.
(38) Kasim, M. S. M.; Sundar, S.; Rengan, R. Synthesis and structure of new binuclear ruthenium(II) arene benzil bis(benzoylhydrazone) complexes: investigation on antiproliferative activity and apoptosis induction. *Inorg. Chem. Front.* **2018**, *5*, 585−596.
(39) Xu, C.-X.; Shen, Y.; Hu, Q.; Zheng, Y.-X.; Cao, Q.; Qin, P. Z.; Zhao, Y.; Ji, L.-N.; Mao, Z.-W. Stabilization of human telomeric G-quadruplex and inhibition of telomerase activity by propeller-shaped trinuclear Pt^{II} complexes. *Chem. - Asian J.* **2014**, *9*, 2519−2526.
(40) Zeng, D.-Y.; Kuang, G.-T.; Wang, S.-K.; Peng, W.; Lin, S.-L.; Zhang, Q.; Su, X.-X.; Hu, M.-H.; Wang, H.; Tan, J.-H.; Huang, Z.-S.; Gu, L.-Q.; Ou, T.-M. Discovery of novel 11-triazole substituted benzofuro[3,2-b]quinolone derivatives as c-myc G-quadruplex specific stabilizers via click chemistry. *J. Med. Chem.* **2017**, *60*, 5407−5423.
(41) Xu, L.; Chen, X.; Wu, J.; Wang, J.; Ji, L.; Chao, H. Dinuclear ruthenium(II) complexes that induce and stabilise G-quadruplex DNA. *Chem. - Eur. J.* **2015**, *21*, 4008−4020.
(42) Taggart, A. K. P.; Teng, S.-C.; Zakian, V. A. Est1p as a cell cycle-regulated activator of telomere-bound telomerase. *Science* **2002**, *297*, 1023−1026.
(43) Qin, Q.-P.; Qin, J.-L.; Meng, T.; Lin, W.-H.; Zhang, C.-H.; Wei, Z.-Z.; Chen, J.-N.; Liu, Y.-C.; Liang, H.; Chen, Z.-F. High in vivo antitumor activity of cobalt oxoisoaporphine complexes by targeting G-quadruplex DNA, telomerase and disrupting mitochondrial functions. *Eur. J. Med. Chem.* **2016**, *124*, 380−392.
(44) Kastan, M. B.; Bartek, J. Cell-cycle checkpoints and cancer. *Nature* **2004**, *432*, 316−323.
(45) Li, R.; Luo, X.; Zhu, Y.; Zhao, L.; Li, L.; Peng, Q.; Ma, M.; Gao, Y. ATM signals to AMPK to promote autophagy and positively regulate DNA damage in response to cadmium-induced ROS in mouse spermatocytes. *Environ. Pollut.* **2017**, *231*, 1560−1568.
(46) Meng, T.; Qin, Q.-P.; Chen, Z.-L.; Zou, H.-H.; Wang, K.; Liang, F.-P. High *in vitro* and *in vivo* antitumor activities of Ln(III) complexes with mixed 5,7-dichloro-2-methyl-8-quinolinol and 4,4′-dimethyl-2,2′-bipyridyl chelating ligands. *Eur. J. Med. Chem.* **2019**, *169*, 103−110.
(47) Qin, Q.-P.; Wang, Z.-F.; Wang, S.-L.; Luo, D.-M.; Zou, B.-Q.; Yao, P.-F.; Tan, M.-X.; Liang, H. *In vitro* and *in vivo* antitumor activities of three novel binuclear platinum(II) complexes with 4′-substituted-2,2′:6′,2″-terpyridine ligands. *Eur. J. Med. Chem.* **2019**, *170*, 195−202.
(48) Pettinari, R.; Marchetti, F.; Condello, F.; Pettinari, C.; Lupidi, G.; Scopelliti, R.; Mukhopadhyay, S.; Riedel, T.; Dyson, P. J. Ruthenium(II)−Arene RAPTA type complexes containing curcumin and bisdemethoxycurcumin display potent and selective anticancer activity. *Organometallics* **2014**, *33*, 3709−3715.
(49) Messori, L.; Casini, A.; Gabbiani, C.; Michelucci, E.; Cubo, L.; Ríos-Luci, C.; Padrón, J. M.; Navarro-Ranninger, C.; Quiroga, A. G. Cytotoxic profile and peculiar reactivity with biomolecules of a novel "rule-breaker" iodidoplatinum(II) complex. *ACS Med. Chem. Lett.* **2010**, *1*, 381−385.
(50) Kwong, W.-L.; Lam, K.-Y.; Lok, C.-N.; Lai, Y.-T.; Lee, P.-Y.; Che, C.-M. A macrocyclic ruthenium(III) complex inhibits angiogenesis with down-regulation of vascular endothelial growth factor receptor-2 and suppresses tumor growth in vivo. *Angew. Chem., Int. Ed.* **2016**, *55*, 13524−13528.

DOI: 10.1021/acsmedchemlett.9b00098
ACS Med. Chem. Lett. 2019, 10, 936−940